European Journal of Medicinal Chemistry 111 (2016) 183–192

Contents lists available at ScienceDirect

European Journal of Medicinal Chemistry

journal homepage: http://www.elsevier.com/locate/ejmech

Research paper

Identification of a new cyathane diterpene that induces mitochondrial and autophagy-dependent apoptosis and shows a potent *in vivo* anti-colorectal cancer activity

Luwei He [a, 1], Junjie Han [a, 1], Baowei Li [b], Li Huang [b], Ke Ma [a], Quan Chen [b], Xinzhong Liu [a], Li Bao [a], Hongwei Liu [a, *]

[a] State Key Laboratory of Mycology, Institute of Microbiology, Chinese Academy of Sciences, Beijing 100101, China
[b] State Key Laboratory of Biomembrane and Membrane Biotechnology, Institute of Zoology, Chinese Academy of Sciences, Beijing 100101, China

ARTICLE INFO

Article history:
Received 22 July 2015
Received in revised form
29 January 2016
Accepted 29 January 2016
Available online 1 February 2016

Keywords:
Fungal diterpene
Cyathin Q
Apoptosis
Autophagy
ATG5 cleavage
ROS

ABSTRACT

Diterpenes has been reported to possess multiple bioactivities consisting of anti-microbial and anti-inflammatory properties. This study reveals a new cyathane-type diterpene (cyathin Q) from the culture of the fungus *Cyathus africanus* by bioactivity-guided separation. The structure of cyathin Q was determined based on spectroscopic measurements (NMR and MS). The bioactivity evaluation shows that cyathin Q has a strong anticancer activity against HCT116 cells and Bax-deficient HCT116 *in vitro* and *in vivo*. This compound induced hallmarks of apoptotic events in HCT116 cells, including caspase activation, cytochrome *c* release, poly (ADP-ribose) polymerase (PARP) cleavage, and depolarization of the mitochondrial inner transmembrane potential. This process is accompanied with the increased mitochondrial ROS, down-regulation of Bcl-2 protein, and up-regulation of Bim protein. We also observed the cleavage of autophagy-related protein ATG5 in cyathin Q-induced apoptosis. Taken together, our study identified a new fungal diterpene that exhibited anticancer activity via induction of mitochondria and autophagy-dependent apoptosis in HCT116 cells.

1. Introduction

Colorectal cancer (CRC) is prevalent due to the bad habits of smoking and alcoholism in the United States [1]. In recent years, CRC has become a worldwide disease with a high rate of mortality [2]. Patients suffering this disease are usually suggested to have surgical resection of the tumor. However, the surgical treatment fails to effectively help the patients because of the metastasis. As alternative treatments, the chemotherapy agents can prolong the survival of the patients and improve the life quality [3].

Natural products contribute greatly to the development of anticancer drugs. It has been estimated that over 48.6% of anticancer drugs in clinics are directly or indirectly derived from natural products [4]. Diterpenes with diverse bioactivities have been identified from plants and fungi [5–7]. Recently, fungi have become a fascinating source for new bioactive secondary metabolites, especially in the field of anticancer compounds [8]. The fungi belonging to the genus of *Cyathus* are unique group of fungi, commonly called as the bird's nest fungi due to their appearance resembling tiny bird's nests filled with “eggs”. A number of biologically active secondary metabolites have been isolated from *Cyathus* sp [9–13].

In our screening for new anticancer agents from fungi, the ethyl acetate extract of the solid culture of *C. africanus* was found to possess strong anti-proliferative effect on colorectal cancer cell line HCT116 *in vitro*. Bioactivity-guided separation led to the isolation of a new cyathane type diterpene (cyathin Q). In this current study, we reported the isolation, structural elucidation, anti-proliferative evaluation, and the action mechanism involving the induction of apoptosis and autophagy in HCT116 cell line. Our work suggests that cyathin Q could serve as a leading compound for new anti-

Abbreviations: Bax, Bcl-2-associated X protein; Bcl-2, B-cell lymphoma/leukemia-2; Bcl-X(L), B-cell lymphoma-extra large; NMR, nuclear magnetic resonance; HRESIMS, high resolution electrospray ionization mass spectroscopy; PARP, poly (ADP-ribose) polymerase; ROS, reactive oxygen species; NOESY, Nuclear Overhauser Enhancement SpectroscopY; AV, Annexin V; PI, propidium iodide; NAC, *N*-acetylcysteine; DTT, (DL-Dithiothreitol); JNK, Jun N-terminal kinase.

* Corresponding author.
E-mail address: liuhw@im.ac.cn (H. Liu).

[1] Luwei He and Junjie Han contributed equally to this work.

http://dx.doi.org/10.1016/j.ejmech.2016.01.056
0223-5234/

cancer drug development.

2. Results and discussion

2.1. Bioactivity-guided isolation of cyathin Q

The ethyl acetate extract (*CA*) prepared from the solid culture of the fungus *C. africanus* was found to be cytotoxic to colorectal cancer cell line HCT116 at the concentration of 25 μg/mL. The ethyl acetate extract was further separated by silica gel column chromatograph to afford ten subfractions. The subfraction-4 and 6 (25 μg/mL) showed strong cytotoxicity towards HCT116 (Fig. 1A). Cyathin Q was obtained from subfraction-4 by crystallization in methanol. The bioactive compounds containing in the subfraction-6 were easily decomposed under room temperature, and thus was not further separated. Furthermore, the viability of HCT116 cells treated with cyathin Q in indicated concentrations was examined by MTT assay. The mean IC_{50} (half maximal inhibitory concentration) exhibited by cyathin Q in HCT116 cells is 9.16 μM (Fig. 1B).

2.2. Structure elucidation of cyathin Q

Cyathin Q was obtained as white powder with the molecular formula of $C_{21}H_{32}O_4$ (6° of unsaturation) as established by high resolution electrospray ionization mass spectroscopy (HRESIMS) and nuclear magnetic resonance (NMR) data (Table 1). A comparison of the ^1H, ^{13}C NMR spectroscopic data of cyathin Q with those of neosarcodonin O [12] suggested that they shared the same cyathane-type skeleton. The HMBC correlations from H3-16 (δ_H, 1.10, 3H, s) to C-5, C-6, C-7, and C-14, from H-21 (δ_H, 3.25, 3H, s) to C-13, from H-13 (δ_H, 4.53, dd, $J = 5.9, 1.1$ Hz) to C-6, C-11, C-14, and C-15, and from H-14 to C-5, C-7, C-13, C-12, and C-16 supported the substitution of a methoxyl group at C-13 and a hydroxyl group at C-14 (Fig. 2A). The coupling constant of 5.9 Hz between H-13 and H-14 suggests the *trans* configuration of these protons, which was also

Table 1
^1H and ^{13}C NMR Data for cyathin Q in CD_3OD.

NO.	Cyathin Q	
	^1H (mult, *J* in Hz)	^{13}C
1	1.53 (m)	38.6
	1.56 (m)	
2	2.31 (m)	29.3
3		140.8
4		140.6
5	2.73 (brd, 12.8)	38.5
6		47.2
7	1.00 (m)	35.8
	2.24 (td, 4.4, 13.3)	
8	1.35 (m)	36.2
	1.60 (m)	
9	3.22 (m)	51.2
10	2.60 (m)	30.3
11	7.18 (m)	160.2
12		144.7
13	4.53 (dd, 1.1, 5.9)	78.5
14	3.62 (d, 5.9)	75.5
15	9.41 (s)	196.2
16	1.10 (s)	17.7
17	1.05 (s)	24.8
18	2.98 (sept, 6.8)	28.5
19	1.01 (d, 6.8)	21.8
20	1.03 (d, 6.8)	22.6
21	3.25 (s)	58.0

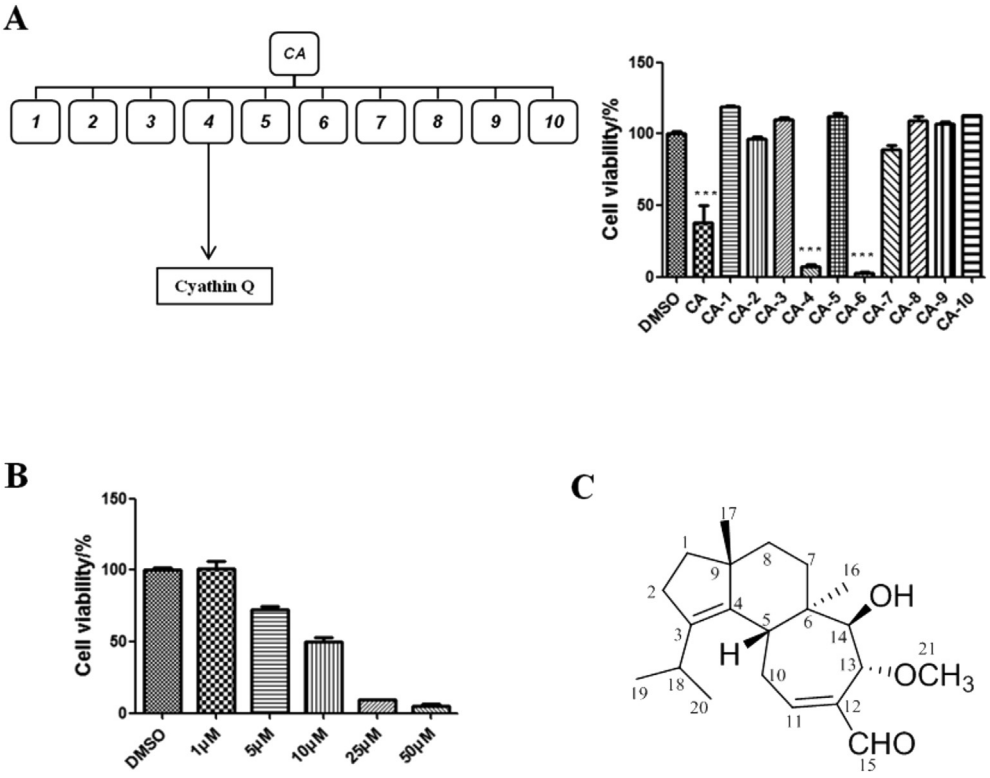

Fig. 1. Bioactivity-guided isolation of cyathin Q. (A) Diagram of compound-screening strategy. HCT116 cells were treated with each fraction of CA-4 in the concentration of 25 μg/mL for 24 h. Viability was analyzed by MTT assay. Viability of cyathin Q treated cells was normalized to untreated cells. Means ± SEM (n = 3). (B) The cytotoxicity of cyathin Q in HCT116 cells. Cells were treated with cyathin Q in the concentration indicated. Viability of cyathin Q was analyzed by MTT assay 24 h later. Viability of cyathin Q treated cells was normalized to untreated cells. Means ± SEM (n = 3). (C) Chemical structure of cyathin Q.

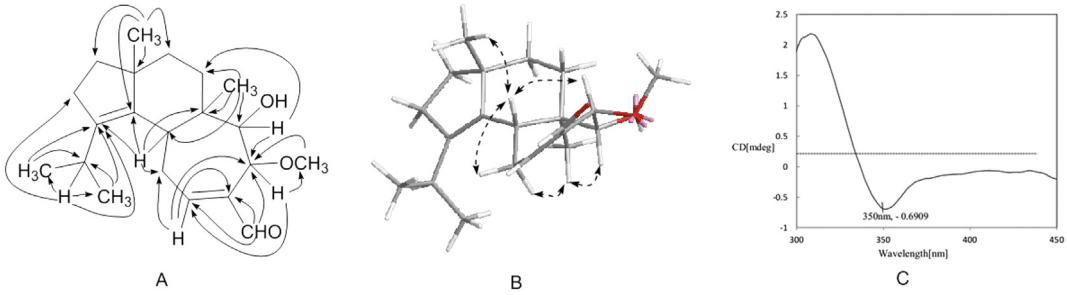

Fig. 2. Key HMBC (A) and NOSEY (B) correlations of compounds 1; CD spectrum of the Rh-complex of 1 with inherent CD spectrum subtracted (C).

supported by the NOESY correlations of H-5 with H-10β, H-13 and H3-17, H3-16 with H-10α and H-14 (Fig. 2B). Accordingly, the structure of cyathin Q was determined. It was the 13-epimer of neosarcodonin O. The absolute configuration of cyathin Q was determined on the basis of the circular dichroism of an in situ formed complex with $[Rh_2(OCOCF_3)_4]$, with the inherent contribution subtracted [14]. On addition of $[Rh_2(OCOCF_3)_4]$ to a solution of cyathin Q in CH_2Cl_2, a metalcomplex was formed as an auxiliary chromophore. It has been reported that the sign of the E band (at ca. 350 nm) can be used to correlate the absolute configuration of a secondary alcohol by applying the bulkiness rule [14,15]. In this study, the Rh complex of cyathin Q displayed a positive E band (Fig. 2C), correlating with 14*R* absolute configuration. Considering the relative configuration determined by NOE data, an absolute configuration of 5*R*, 6*R*, 9*R*, 13*R*, and 14*R* was assigned to cyathin Q. Thus, the structure of cyathin Q was elucidated as shown in Fig. 1C.

2.3. Cyathin Q induces apoptosis in HCT116 cells

Apoptosis is a process of programmed cell death which clears the aging and damaged cells normally. However, cancer cells usually have an abnormal ability of proliferation mainly due to the defective apoptosis and the dysregulated cell cycle [16]. Thus, activation of apoptosis can be a therapy for cancer by reducing accumulation of cancer cells. To determine whether cyathin Q-induced cytotoxicity in HCT116 cells could be, at least in part, the result of cell apoptosis, we examined the induction effect of cyathin Q on cell apoptosis of HCT116 by annexin-V/PI staining method and immunofluorescence. Notably, cyathin Q induced the apoptosis in HCT116 cells in a time and dose-dependent manner. When HCT116 cells were treated with cyathin Q at the concentration of 10 μM for 24 h, the proportion of apoptotic cells reached 82.07% (Fig. 3A). The structure of cyathin Q is very similar with that of neosarcodonin O except for the relative configuration at C-13. With neosarcodonin O in hand [17], we compared the apoptosis-inducing activity between cyathin Q and neosarcodonin O by annexin-V/PI staining analysis. And this data shows that cyathin Q has much stronger anticancer activity than neosarcodonin O (Cisplatin was used as positive control, SI.3A), which reveals the greater influence of the configuration of the methoxyl group at C-13 on apoptosis-inducing activity.

Moreover, we found that cyathin Q showed somewhat selectivity in inducing the apoptosis in colorectal cancer cells HCT116 and SW480 cells (Fig. 3B). Since colorectal cells were more sensitive to cyathin Q, we used HCT116 cells as a model to investigate the anticancer activity and action mechanism of cyahtin Q. To confirm the apoptosis event, we further detected the caspase activity, the cleavage of PARP protein, and the release of cytochrome *c*. Cyathin Q induced caspase activation in a time-dependent manner (Fig. 3C). The pan-caspase inhibitor Z-VAD-FMK strongly inhibit apoptosis induced by cyathin Q. Z-VAD-FMK (50 μM) decreased the proportion of apoptotic cells from 70.02% to 28.81% (Fig. 3D). In the meanwhile, the cleavage of PARP was detected (Fig. 5). Cytochrome *c* release from mitochondria to cytoplasm was observed by immunofluorescence assay (Fig. 3E). As we know, apoptosis is divided into two general pathways including intrinsic and extrinsic pathways. The intrinsic pathway mainly depends on mitochondria events including loss of mitochondria membrane potential and release of pro-apoptotic protein like cytochrome *c* from intermembrane to cytosol [18]. Therefore, the cell apoptosis induced by cyathin Q is involved in the intrinsic apoptotic pathway.

2.4. Cyathin Q induced the increase of ROS and JNK activation

Excess reactive oxygen species (ROS) triggered by external stimuli can activate apoptosis [19]. As cyathin Q had induced obvious apoptosis on HCT116 cells, we examined the level of ROS and mitochondrial superoxide (Mito-SOX) by flow cytometry analysis. Results indicated that cyathin Q elevated overall cellular ROS and the mitochondrial superoxide radical in HCT116 cells in a dose-dependent manner (Fig. 4A, B). Moreover, both the ROS scavenger NAC and the reductant DTT (DL-Dithiothreitol) can inhibit apoptosis induced by cyathin Q(5 μM, 24 h) as shown by annexin-V/PI staining analysis (Fig. 4C). We also found the oxidative stress induced by cyathin Q in HCT116 cells can active JNK pathway. JNK activation acts a central role in ROS and oxidative stress inducing apoptosis. Once triggered by stimuli, JNK translocates to mitochondria and then modulate the activities of mitochondrial pro- and anti-apoptotic proteins through phosphorylated modification [20]. As shown in Fig. 3E, when HCT116 cells were treated with cyathin Q (5 μM) for indicated times, the phosphorylated JNK was increased in four hours of the treatment. At the same time, cyathin Q induced an obvious loss of mitochondrial membrane potential ($\Delta\psi m$) in a dose-dependent manner (Fig. 4D). Mitochondrial oxidative phosphorylation inhibitor (FCCP) which can obviously decrease mitochondrial membrane potential was used as a positive control. From above on these data, we conclude that cyathin Q induced ROS-mediated apoptosis in HCT116 cells with changing cellular redox state and inducing the depolarization of the mitochondrial inner transmembrane potential.

2.5. Cyathin Q made effect on Bcl-2 family proteins

Bcl-2 family proteins play a very important role in the regulation of cell apoptosis [21,22]. The pro-apoptotic protein Bax and Bak can be recruited to mitochondrion and trigger cytochrome *c* release into cytoplasm to activate caspase cascade. While anti-apoptotic proteins of Bcl-2 family, such as Bcl-2 and Bcl-X(L), can inhibit the function of pro-apoptotic proteins by interaction [16,23,24]. Cancers with high levels of Bcl-2 or Bcl-X(L) show drug resistance in clinical cancer treatment. In addition, Bim as one of BH3-only proteins can directly activate Bax to trigger apoptosis [25].

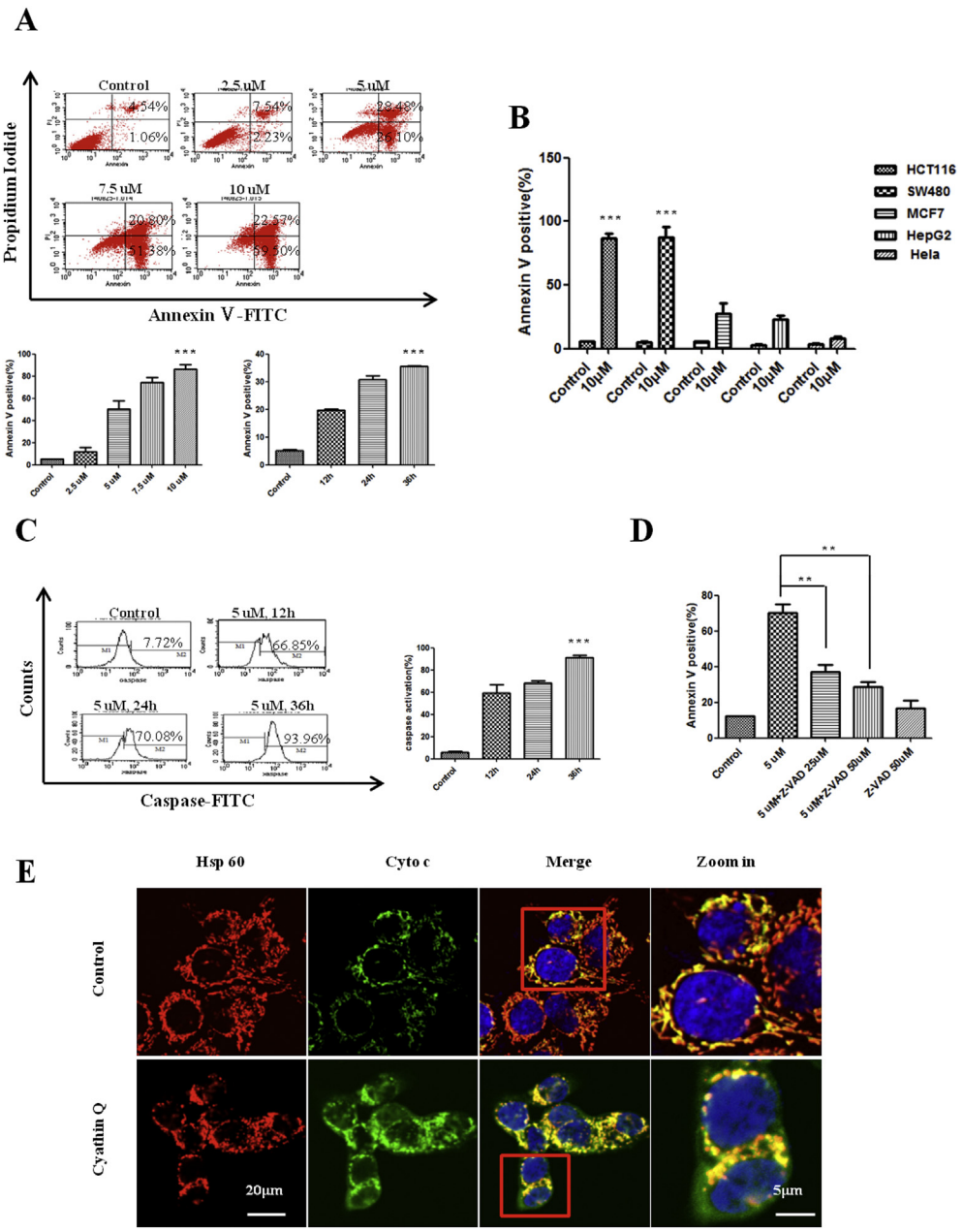

Fig. 3. CyathinQ induces apoptosis in HCT116 cells. (A) Five different cancer cells were treated with cyathin Q (10 μM, 24 h). The rate of apoptosis was analyzed by flow cytometry through annexin V/PI staining. Means ± SEM (n = 3). (B) HCT116 cells were treated with cyathin Q in the concentration indicated for 24 h. And cyathin Q treated HCT116 for indicated times. The rate of apoptosis was analyzed by flow cytometry through annexin V/PI staining. Means ± SEM (n = 3). (C) Cyathin Q treated HCT116 cells at the concentration of 5 μM for indicated times. Then the cells were stained with CASPACEFITC-conjugated caspase marker for flow cytometry analysis. Means ± SEM (n = 3). (D) HCT116 cells were pre-treated with Z-VAD-FMK caspase inhibitor (1 h), and then incubated with cyathin Q (5 Mm, 24 h). The rate of apoptosis was analyzed by flow cytometry through annexin V/PI staining. Means ± SEM (n = 3). (E) HCT116 cells were treated with 5 μM cyathin Q for 12 h and then analyzed by immunohistochemistry using anti-cytochrome *C* antibodies, with nuclei stained with DAPI and mitochondria with Hsp 60. Cells were visualized by confocal microscopy. The zoom-in images on the right are from the boxed areas. Scale bars = 20 μm.

In order to investigate the effects of cyathin Q on apoptosis-related proteins in the intrinsic (mitochondrial) pathway, we assessed Bcl-2, Bcl-X(L), Bax, Bim, and p53 protein by western blot [26,27]. In the treatment of cyathin Q, the expression of Bcl-2 greatly decreased and all three isoforms of Bim increased. The expression level of Bcl-X(L), Bax, and p53 remained unchanged (Fig. 5). Further, we checked the effect of cyathin Q on Bcl-2 gene expression by quantitative real-time PCR. To our surprise, cyathin Q induced the increase of Bcl-2 gene expression (SI.3B). Therefore, the decrease of Bcl-2 protein induced by cyathin Q might be due to the post-translational modification. This modification may be caused by ubiquitination. It need be further researched.

Above all, the down-regulation of Bcl-2 and up-regulation of Bim is involved in the cyathin Q-induced apoptotic process.

2.6. Cyathin Q induced apoptosis in bax-deficiency HCT116 cell line

Bax is a very important apoptotic protein mediating the apoptotic release of cytochrome *c* from mitochondria. *Bax*-deficiency or mutation in cancer cells can lead to drug resistance in

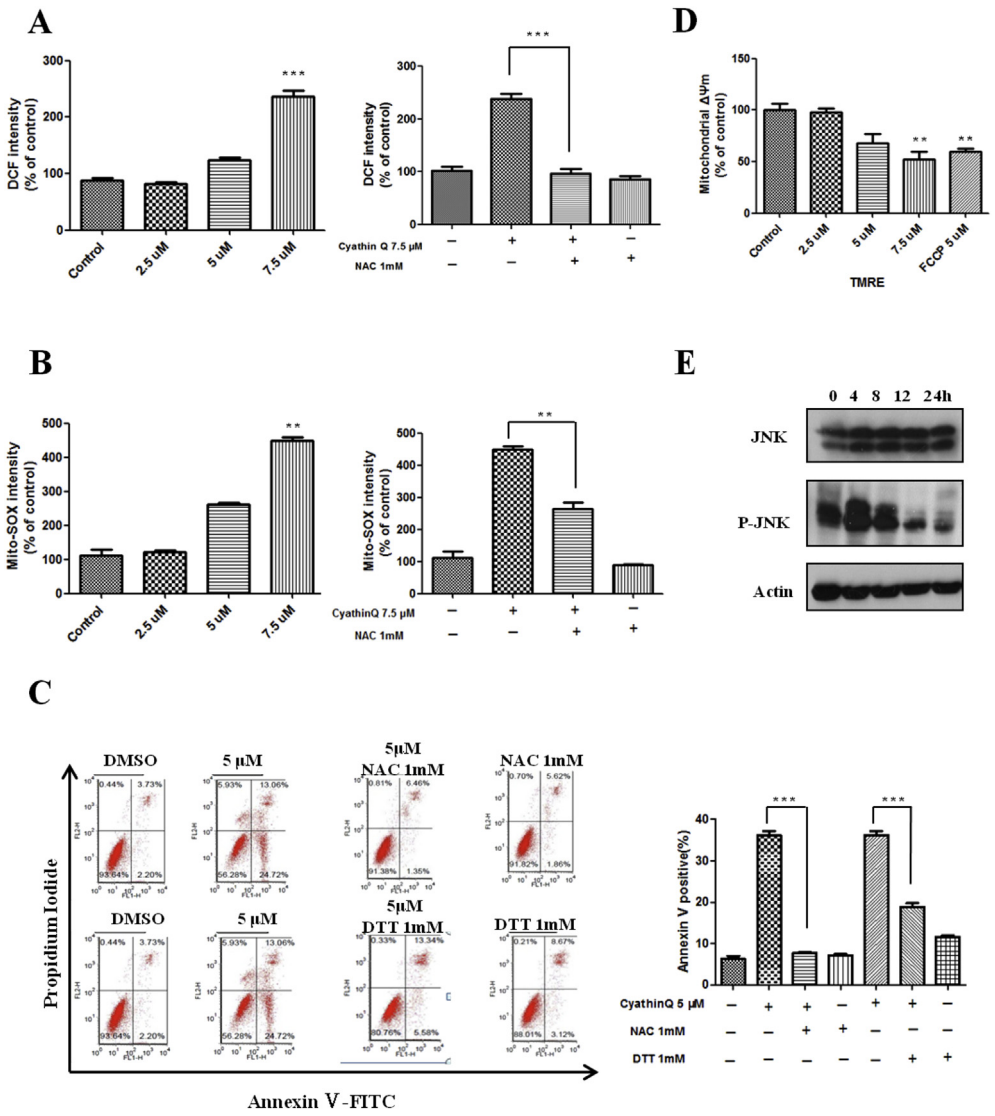

Fig. 4. Cyathin Q induced the increase of ROS and JNK activation. (A–B) HCT116 cells were pre-treated (1 h) with NAC followed by: (A) Cells were incubated with cyathin Q (6 h) then stained with H2DCFDA and analyzed by flow cytometry. Means ± SEM (n = 3). (B) Incubation with cyathin Q (5 μM, 16 h). The cells were stained with MitoSOX Red ROS indicator and analyzed by flow cytometry. Means ± SEM (n = 3). (C) HCT116 cells were pre-treated (1 h) with NAC or DTT followed by: cells were incubated with cyathin Q (5 μM, 24 h), and analyzed for apoptosis by annexin V/PI staining. Means ± SEM (n = 3). (D) HCT116 cells were treated with cyathin Q (5 μM, 6 h) or FCCP (10 μM, 6 h) as positive control, incubated with TMRE (10 min, 37 °C), and fluorescence which represents mitochondrial membrane potential (ψm) was analyzed by flow cytometry. Means ± SEM (n = 3). (E) HCT116 cells were treated with cyathin Q for indicated times. Then the whole cell lysates were analyzed by western blotting with anti-JNK, and anti-JNK-P antibodies. Actin was used as loading control.

cancer therapy [28,29]. There have been increasing numbers of researches studying the mechanism and anticancer effects of compounds inducing Bax-independent apoptosis in cancer cells [30–32]. Surprisingly, cyathin Q effectively suppressed the viability of $Bax^{-/-}$ HCT116 cells (Fig. 6A). The mean IC_{50} (half maximal inhibitory concentration) exhibited by cyathin Q in $Bax^{-/-}$ HCT116 cells is 24.16 μM. Furthermore, we also analyzed the apoptosis of $Bax^{-/-}$ HCT116 cells treated with cyathin Q in indicated concentrations by annexin-V/PI staining. As shown in the Fig. 6B, the apoptosis induced by cyathin Q in $Bax^{-/-}$ HCT116 cells was in a dose-dependent manner. Moreover, ROS scavenger NAC and the reductant DTT can inhibit the cyathin Q induced apoptosis (Fig. 6C). It was confirmed that the apoptosis induced by cyathin Q in $Bax^{-/-}$ HCT116 cells was mediated by ROS. Cyathin Q can be a leading compound which antagonizes the chemoresistance caused by down-regulation of Bax protein.

2.7. ATG 5 cleavage during cyathin Q-induced apoptosis in HCT116 cells

Autophagy is a catabolic process functioning in degradation of misfolded proteins and dysfunctional organelles. Normally autophagy exists as a protective mechanism in cells, while persistent activation of autophagy by toxic agent will lead to cell death [33]. In our experiment, cyathin Q was found to induce autophagy at the dose of 5 μM. It was shown that cyathin Q increased the level of LC3-II, the biochemical hallmark of autophagy (Fig. 7A) [34]. As increased LC3-II levels can occur when autophagy is either induced or inhibited, the autophagy-inducing activity of cyathin Q needs further confirmation. Chloroquine, an inhibitor of autophagy, is a well-known lysosomotropic agent playing a role in accumulating acid vesicular organelles in the late phase of autophagy [35]. It is usually used for evaluation of autophagic flux. In current study,

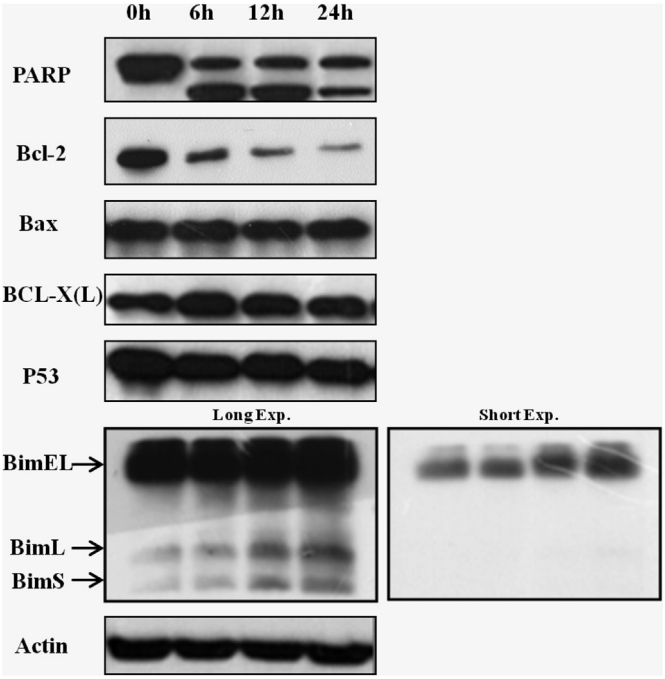

Fig. 5. Cyathin Q induced down-regulation of Bcl-2 proteins. HCT116 cells were treated with 5 μM cyathin Q for the indicated times, and the apoptosis-related protein were analyzed by Western-blotting.

chloroquine increased the LC3-II level (Fig. 7B) in cyathin Q treated HCT116 cells, suggesting that cyathin Q was able to induce autophagic flux. In addition, we examined the expression level of Beclin1 and ATG5 proteins. The protein Beclin1 participates in initial step of autophagy, and ATG5 is required for elongation and conjugation of autophagosomes by conjugating with ATG12 [36]. Recent researches have indicated that autophagy-related genes ATG-5 and Beclin 1 actively participate in the regulation of apoptosis. The cleavage product of Beclin 1 or ATG5 can provoke apoptotic cell death [37–40]. Western blotting analysis of cells treated with cyathin Q indicated that the level of Beclin 1 remained unchanged, the expression of ATG5 was increased, and the cleavage of ATG5 occurred (Fig. 7A). The antibody to ATG5 used in our experiment can recognize ATG5-ATG12 complex (50KD) and free ATG5 (33KD). Our data shows remarkable cleavage of free ATG5 (24KD). To further confirm the role of ATG5 in the cyathin Q induced apoptosis. We constructed a stable ATG5 knockdown HCT116 cell lines by RNA interference (Fig. 7C). Knockdown of ATG5 in HCT116 cells drastically reduced the apoptosis of cells under the treatment of cyathin Q (5 μM, 24 h, Fig. 7D). It has been reported that the cleavage of ATG5 has the function of switching autophagy to apoptosis and provoking apoptotic cell death [37–40]. In order to confirm the effect of ATG5 cleavage by cyathin Q, we used the autophagy inhibitor (chloroquine) and apoptosis inhibitor (Z-VAD-FMK) to block the ATG5 cleavage. It is shown that chloroquine remarkably blocked the ATG5 cleavage and Z-VAD-FMK slightly blocked this cleavage (SI.3C). Thus, we speculate that the effect of cyathin Q on ATG5 cleavage directly correlate with autophagy induction. Based on above results, ATG5 is essential for apoptosis induced by cyathin Q.

2.8. *In vivo* anticancer activity

We used a xenograft mouse model to examine the *in vivo* anticancer effect of cyathin Q. Wild type HCT116 cancer cells and $Bax^{-/-}$ HCT116 cells were implanted into nude mice respectively and tumor growth was monitored after one week. Animals developed tumors with an average volume of 0.117 cm^3. The mice were divided in three groups and treated intraperitoneally (i.p.) either with vehicle or with cyathin Q (5 or 10 mg/kg) for 14 days. As shown in Fig. 8, cyathin Q effectively inhibited the growth of wild type HCT116 colon cancer cells and $Bax^{-/-}$ HCT116 cells after two weeks. In vehicle-treated mice, the volume of tumor with HCT116 cells increased from 0.117 cm^3 to 1.632 cm^3 in 14 days. Cyathin Q (5 or 10 mg/kg), for two weeks inhibited xenograft tumor sizes by 26.0% and 62.2%, respectively when compared to vehicle control. For mice implanted into $Bax^{-/-}$ HCT116 cells, cyathin Q (5 and 10 mg/kg) also inhibited the growth of tumor by 25.8% and 60.1% in contrast with vehicle control. During the period of treatment, there was no obvious weight loss (SI.1) or discomfort behavioral changes, and no obvious tissue damages on liver function in the cyathin Q treated group (SI.2). The advantages of cyathin Q lies on its strong anticancer effect *in vivo* and little side effects.

3. Conclusion

A new fungal diterpene cyathin Q was isolated from the solid culture of the fungus *Cyathus africanus*. Cyathin Q can suppress the growth of colon cancer cells HCT116 and *bax*-deficiency HCT116 cells both *in vivo* and *in vitro*. The elevated level of ROS is crucial for apoptosis induced by cyathin Q. Interestingly, autophagy simultaneously occurred in the HCT116 cells treated with cyathin Q, and cyathin Q induced the cleavage of ATG5. Down regulation of Bcl-2 protein is also involved in the apoptotic process. Based on all the data shown in this study, we suggest that cyathin Q could be a potential drug for colorectal cancer therapy.

4. Experimental section

4.1. Chemistry

4.1.1. Instruments and reagents

Solvent used for extraction and chromatographic separation was analytical grade. TLC was carried out on Silica gel $HSGF_{254}$ and the spots were visualized by spraying with 10% H_2SO_4 and heating. Silica gel (Qingdao Haiyang Chemical Co., Ltd., People's Republic of China), ODS (Lobar, 40–63 μm, Merck), and Sephadex LH-20 (Amersham Biosciences) were used for column chromatography. HPLC separation was performed on an Waters 2998 HPLC system using an ODS column (C_{18}, 250 × 10 mm, YMC Pak, 5 μm; detector: UV) with a flow rate of 1.0 mL/min. IR spectral data was acquired using a Nicolet IS5 FT-IR spectrophotometer, respectively. Optical rotations were measured on an Anton Paar MCP 200 Automatic Polarimeter. NMR spectral data were obtained with Bruker Avance-500 spectrometer using solvent signals (CD_3OD, δ_H 3.30/δ_C 49.9) as references. The HSQC and HMBC experiments were optimized for 145.0 and 8.0 Hz, respectively. HRESIMS data were measured using an Agilent Accurate-Mass-Q-TOF LC/MS 6520 instrument.

4.1.2. Extraction and isolation of cyathin Q

The strain of *C. africanus* was isolated from the fruiting body of *C. africanus* collected in the Linzhi region of Tibet Plateau. The fungus was deposited in China General Microbiological Culture Collection (CGMCC 8411). Firstly, *C. africanus* was cultured on slants of PDA media at 25 °C for 7 days. Then, Agar plugs were inoculated in 500 mL Erlenmeyer flask containing 180 mL of PDB media (0.4% glucose, 1% malt extract, and 0.4% yeast extract; the final pH of the media was 6.5) before sterilization, and incubated at 25 °C on a rotary shaker at 160 rpm for 7 days. The strain was incubated on rice in fifty 500 mL Fernbach flasks at 25 °C for 38 days to afford the

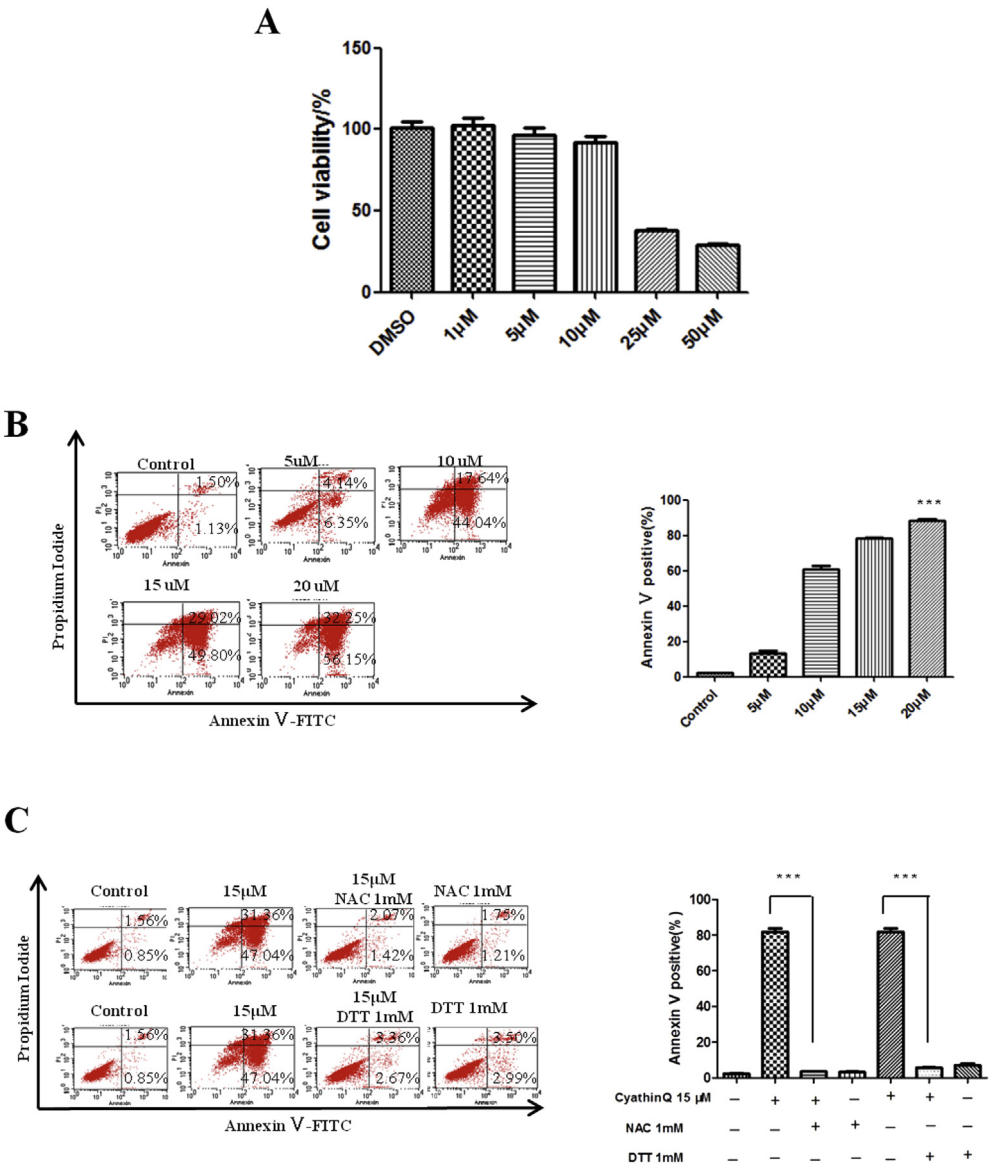

Fig. 6. Cyathin Q induced apoptosis in bax-deficiency HCT116 cell line. (A) The cytotoxicity of cyathin Q in Bax-deficient HCT116 cells. Cells were treated with cyathin Q in the concentration indicated. Viability of cyathin Q was analyzed by MTT assay 24 h later. Viability of cyathin Q treated cells was normalized to untreated cells. Means ± SEM (n = 3). (B) Bax-deficient HCT116 cells were treated with cyathin Q in the concentration indicated for 24 h. And cyathin Q treated HCT116 for indicated times. The rate of apoptosis was analyzed by flow cytometry through annexin V/PI staining. Means ± SEM (n = 3). (C) Bax-deficient HCT116 cells were pre-treated (1 h) with NAC or DTT followed by: cells were incubated with cyathin Q (5 μM, 24 h), and analyzed for apoptosis by annexin V/PI staining. Means ± SEM (n = 3).

solid culture. Each flask contains 80 g of rice and 100 mL of distilled water.

The culture was extracted repeatedly with ethyl acetate by exhaustive maceration (3 × 3 L), and the organic solvent was evaporated to dryness under vacuum to afford the crude extract (25.8 g). The ethyl acetate extract was subjected to a silica gel column chromatography (CC) eluted with a gradient of *n*-hexane-ethyl acetate (*v*/*v*, 100:0, 100:1, 100:2, 100:5, 100:10, 100:15, 100:25, 100:35) and dichloromethane-acetone (*v*/*v*, 100:2, 100:4, 100:8, 100:15, 100:25, 100:35, 0:100) to give eleven fractions (*CA*-1–*CA*-11). Fractions *CA*-4 eluted with *n*-hexane-ethyl acetate (*v*/*v*, 100:15) exhibited strong anti-proliferative activity against HCT116 cells. Cyathin Q (152 mg) was obtained from the fraction *CA*-4 by recrystallization in methanol.

Cyathin Q: White powder ($CHCl_3$); [α]25 D-165 (*c* 0.13, MeOH); UV (MeOH) λ_{max} (log ε) 203 (3.90) nm, 235 (3.32) nm; IR (ν_{max}): 3439, 2932, 2846, 1738, 1681, 1456, 1375, 1179 cm^{-1}; ^1H NMR and ^{13}C NMR, see Table 1; Positive HRESIMS *m*/*z* 355.2239 $[M + Na]^+$ (calcd. For $C_{21}H_{32}O_3Na$, 355.2244).

4.1.3. Absolute configuration of cyathin Q

According to a published procedure, 0.5 mg of compound tested (cyathin Q) was dissolved in a dry solution of the stock [Rh_2(O-$COCF_3)_4$] complex (1.5 mg) in CH_2Cl_2 (200 μL) and was subjected to CD measurements at a concentration of 2.5 mg/mL. The first CD spectrum was recorded immediately after mixing, and its time evolution was monitored until stationary (about 10 min after mixing). The inherent CD was subtracted. The observed sign of the E band at ca. 350 nm in the induced CD spectrum was correlated to the absolute configuration of the secondary alcohol moiety.

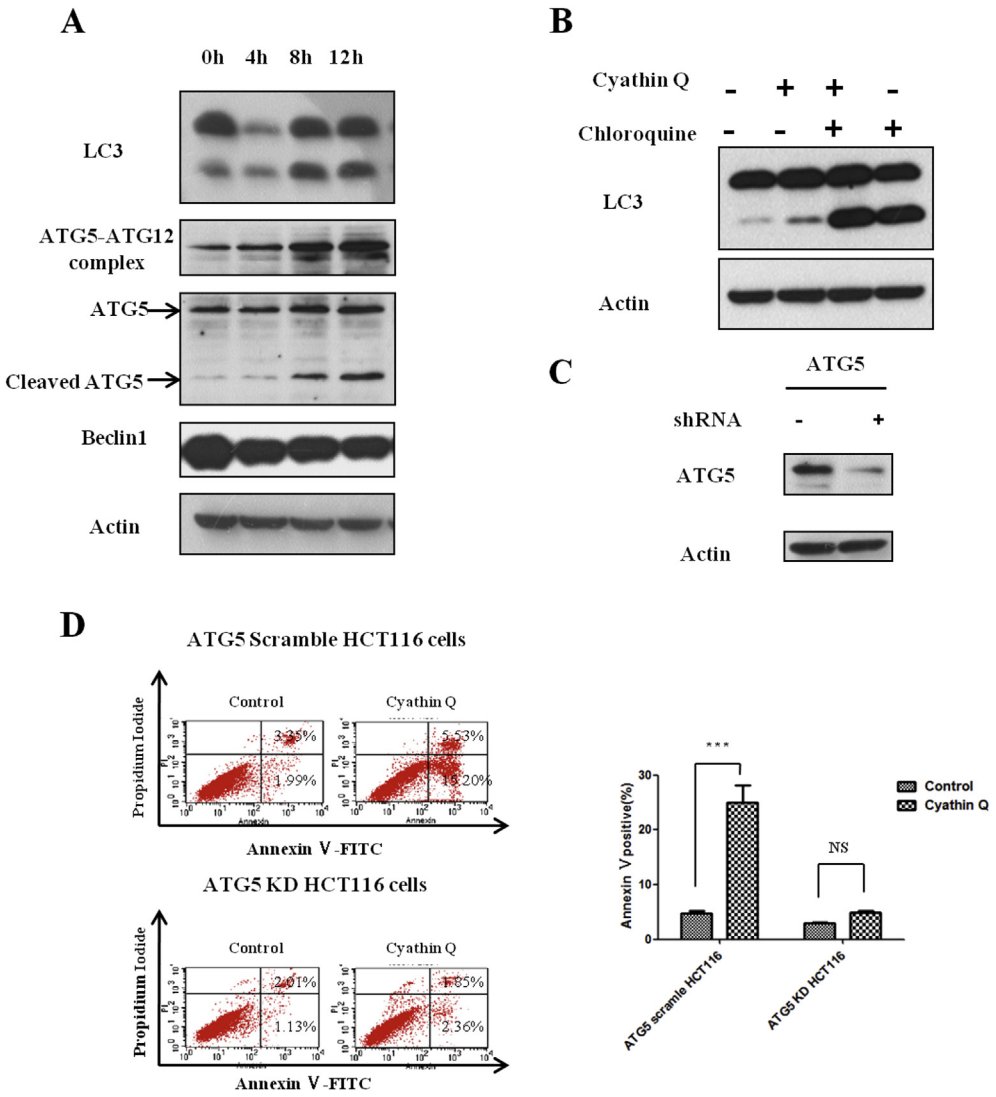

Fig. 7. ATG 5 cleavage during cyathin Q-induced apoptosis in HCT116 cells. (A) HCT116 cells were treated with cyathin Q (5 μM) for indicated times. Then the whole cell lysates were analyzed by western blotting with anti-LC3, anti-Beclin 1, and anti-Atg 5 antibodies. Actin was used as loading control. (B) HCT116 cells were treated with cyathin Q with or without chloroquine, respectively. Then the whole cell lysates were analyzed by western blotting with anti-LC3 antibodies. Actin was used as loading control. (C) HCT116 cells were transfected of ATG5 siRNA or the scramble siRNA. Then these two cells were screened by G418 to be stable cell lines. (D) ATG5 scramble cells and ATG5 KD cells were incubated with cyathin Q (5 μM, 24 h), and analyzed for apoptosis by annexin V/PI staining. Means ± SEM (n = 3). Schematic summary of cell death induced by cyathin Q is on the right.

4.2. Pharmacology and biochemistry

4.2.1. Reagents

The following reagents involved in this research: 3-(4,5-dimethylthiazol-2-yl)-2,5-diphenyltetrazolium bromide (MTT), the chloroquine, the ROS scavenger NAC, the reductant DTT were purchased from Sigma; the ROS indicator DCF, the mitochondrial ROS indicator Mito-SOX, and the mitochondrial dye TMRE were purchased from Invitrogen (Grand Island, NY).

Antibodies to ATG5 was from Abgent (San Diego, CA), to β-actin, Bim, LC3 were from Sigma (St. Louis, MO), to Bcl-2, Bcl-xL, Beclin, cytochrome *C*, PARP, Tim23 and Tom20 were from BD Biosciences(San Jose, CA). Anti-JNK, anti-JNK-P and anti-Hsp60 were from Cell Signaling Technology (Danvers, MA). Bax, P53, FITC-conjugated goat anti-mouse and anti-rabbit antibodies were from Santa Cruz Biotechnology (Santa Cruz, CA). HRP-labeled anti-rabbit IgG and goat anti-mouse antibodies were from Kirkegaard & Perry Laboratories. Goat anti-mouse IgG Alexa Fluor-568 (Molecular Probes, Eugene, Oregon) was used for the Cy3-conjugated secondary antibodies in immunofluorescence.

4.2.2. Cell culture

HCT116 cells, E1A- and K-Ras-transformed Bax$^{-/-}$ HCT116, SW480 cells, MCF7 cells, HepG2 cells and HeLa cells were cultured in DMEM supplemented with 10% heat inactivated fetal bovine serum (FBS), 100 μg/mL streptomycin and 100 U/mL penicillin in 5% CO_2 at 37 °C.

4.2.3. Cell viability assay

The cytotoxicity effect of cyathin Q on HCT116 cells and Bax$^{-/-}$ HCT116 cells was determined by MTT assay. Cells (1×10^4 cells/well) were seeded in a 96-well plate, and treated with cyathin Q or the each fraction of crude extract CA. MTT which is described before was added in the plate after incubated for 24 h. Then MTT containing medium was washed, the crystals that had formed were dissolved by the addition of DMSO to each well. The absorbance of the cells was measured at 560 nm after dissolving absolutely by using Multiskan Spectrum Microplate Reader.

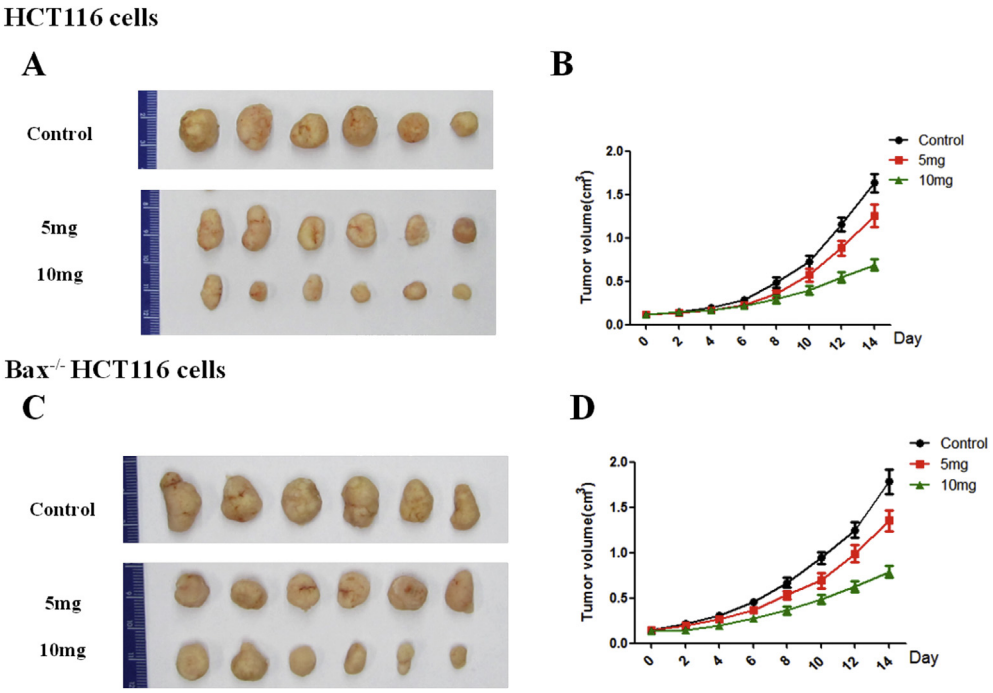

Fig. 8. In vivo anticancer activity. Immune-deficient nude mice were implanted with HCT116 cells (A–B) or Bax-deficient HCT116 cells (C–D), respectively. One week later, the mice were divided into 3 groups (6 mice/group) and underwent intra-peritoneal treatment with the vehicle control (DMSO, 10%) or cyathin Q (5 or 10 mg/kg/2 days) for 2 weeks, during which time tumor size was measured. Two weeks post-cyathin Q treatment, the mice were euthanized and the xenografts were excised for further studies. Tumor volume curves (B, D) and representative images of isolated tumors (A, C) and average body weights of nude mice after two weeks of treatment (SI.1) are shown.

4.2.4. Detection of apoptosis

According to the recommended protocol, the apoptosis of apoptotic cell death was analyzed by annexin V-FITC and PI staining based on apoptosis detection kit (PharMingen) through flow cytometry. Caspase activity of treated cells was examined by a CaspACEFITC-VAD-FMK kit. Flow cytometry data were obtained with FACScan and analyzed with CellQuest software (BD Biosciences).

4.2.5. ROS and mitochondrial superoxide detection

HCT116 cells (5×10^5 cells/mL) were incubated with cyathin Q in the indicated concentrations for the indicated times. Then these cells were harvested, washed with PBS and incubated with carboxy-H2DCFDA (37 °C, 10 min) to detect ROS. Fluorescence intensity in the cells was analyzed by FACS, with excitation set at 488 nm. While cells were incubated with MitoSOX Red (37 °C, 30 min), and fluorescence was measured with excitation at 510 nm for mitochondrial superoxide detection. The data were analyzed with Cell Quest software (BD Biosciences, San Jose, CA).

4.2.6. Measurement of mitochondrial membrane potential

HCT116 cells (5×10^5 cells/mL) were treated with cyathin Q in indicated concentrations for 24 h to determine ψm. Carbonyl cyanide 4-(trifluoromethoxy) phenylhydrazone (FCCP; proton gradient uncoupler) was used for a positive control. Then cells were washed twice with PBS, and TMRE was added to the cells at 37 °C for 10 min. The amount of TMRE retained by 10,000 cells per sample was measured at 590 nm (red fluorescence, FL-2) with a FACScan flow cytometer and analyzed with Cell Quest software (BD Biosciences, San Jose, CA).

4.2.7. Knock-down of ATG5 expression

The scramble RNA interference sequence is 30-GACATTTGTAACGGGATTC-50; the target sequence in ATG5 is 50-GAAGTTTGTCCTTCTGCTA-30. According to the manufacturer's instructions (Ambion), Primers for short hairpin RNA were designed, and cloned into the pSilencer2.1-neo vector. HCT116 cells were transfected with the corresponding vectors and selected with G418.

4.2.8. Western blot

Cells were harvested and lysed by cell lysis buffer (20 mM Tris, 2 mM EGTA, 1% NP-40, pH 7.4) supplemented with protease inhibitor PMSF after the certain transfection or treatment. Equivalent protein quantities (20 μg) were resolved by SDS-PAGE and transferred to nitrocellulose membranes. Membranes were blocked with PBS containing 5% nonfat milk and 0.1% Tween-20 for 1 h at room temperature subsequently, incubated with the corresponding primary antibodies. Immunoreactive bands were visualized with a chemiluminescence kit (ThermoFisher, Waltham, MA) followed by incubation with HRP-conjugated secondary antibodies.

4.2.9. Immunofluorescence assay

Firstly, cells were seeded in the 6-well plate with sterilized coverslips. After indicated treatment, cells were fixed by 3.7% formaldehyde in DMEM for 15 min at 37 °C. With PBS buffer containing 0.2% Triton X-100The fixed, cells were permeabilized for 15 min on ice. Then cells were blocked by PBS buffer containing 2% BSA and incubated with indicated primary antibodies for 1 h at room temperature. Cell images were captured with an LSM 510 Zeiss confocal microscope (Carl Zeiss Jena, Germany) followed by the incubation of fluorescence-conjugated secondary antibodies at room temperature for 1 h.

4.2.10. Xenograft experiments using nude mice

$Bax^{-/-}$ HCT116 and HCT116 colon cancer cells (5×10^5) were subcutaneously injected into the back of the upper limbs of 4–5 weeks old nude BALB/C mice. Then the mice were separated into three groups (6 mice/group). One week post-injection, two groups

were treated with 5 or 10 mg/kg cyathin Q, while the third group as a vehicle control was treated with DMSO (50% (*v*/*v*) in 1.8% NaCl) every other day for two weeks. After this treatment, three groups of mice were sacrificed and tumors were excised. According to the formula $V = a \times b^2/2$, tumor length (a) and width (b) measured using a slide gauge can acquire tumor volumes (V). Mice were maintained in specific pathogen-free conditions and all research work was approved by the Animal Care and Use Committee of the Institute of Zoology, Chinese Academy of Sciences.

4.2.11. Statistical analysis

Statistical evaluation was carried out using Student's *t*-test (two-tailed) to test for differences between control and experimental results. Data are expressed as means ± SEM. Following the nonparametric Mann–Whitney *U* test, the level of significance of differences between control and treated samples was determined. When the P value was deemed <0.05 (*), <0.01 (**), or <0.001 (***), a difference was considered statistically significant. Tumor volume data were analyzed using one-way repeated measures analysis of variance.

Acknowledgements

Financial supports of the National Nature Science Foundation (21472233) and the Ministry of Science and Technology of China (2014CB138304) are acknowledged. Dr. Jinwei Ren (State Key Laboratory of Mycology, Institute of Microbiology, Chinese Academy of Sciences) is appreciated for their help in measuring the NMR data. We also thank Mrs. Jing Wang (State Key Laboratory of Biomembrane and Membrane Biotechnology, Institute of Zoology, Chinese Academy of Sciences) for operating the flow cytometer.

Appendix A. Supplementary data

Supplementary data related to this article can be found at http://dx.doi.org/10.1016/j.ejmech.2016.01.056.

References

[1] I. Vogelaar, et al., How much can current interventions reduce colorectal cancer mortality in the U.S.? Mortality projections for scenarios of risk-factor modification, screening, and treatment, Cancer 107 (7) (2006) 1624–1633.
[2] R. Siegel, C. Desantis, A. Jemal, Colorectal cancer statistics, 2014, CA Cancer J. Clin. 64 (2) (2014) 104–117.
[3] P.C. Simmonds, Palliative chemotherapy for advanced colorectal cancer: systematic review and meta-analysis. Colorectal Cancer Collaborative Group, BMJ 321 (7260) (2000) 531–535.
[4] D.J. Newman, G.M. Cragg, Natural products as sources of new drugs over the 30 years from 1981 to 2010, J. Nat. Prod. 75 (3) (2012) 311–335.
[5] A.K. Bhattacharya, et al., Clerodane type diterpene as a novel antifungal agent from *Polyalthia longifolia* var. pendula, Eur. J. Med. Chem. 94 (2015) 1–7.
[6] R.M. Young, et al., Antiplasmodial activity: the first proof of inhibition of heme crystallization by marine isonitriles, Eur. J. Med. Chem. 93 (2015) 373–380.
[7] F. Olmo, et al., Prospects of an alternative treatment against *Trypanosoma cruzi* based on abietic acid derivatives show promising results in Balb/c mouse model, Eur. J. Med. Chem. 89 (2015) 683–690.
[8] D.D. De Silva, et al., Bioactive metabolites from macrofungi: ethnopharmacology, biological activities and chemistry, Fungal Divers. 62 (1) (2013) 1–40.
[9] Wojciech Krzyczkowski, E.M. Franciszek Herold, The structure, medicinal properties and biosynthesis of cyathane diterpenoids, Biotechnologia 1 (80) (2008) 146–167.
[10] J.W. Shen, Y. Ruan, B.J. Ma, Diterpenoids of macromycetes, J. Basic Microbiol. 49 (3) (2009) 242–255.
[11] D.L. Wright, C.R. Whitehead, Recent progress on the synthesis of cyathane type diterpenes. A review, Org. Prep. Proced. Int. 32 (4) (2000) 307–330.
[12] T. Kamo, et al., Anti-inflammatory cyathane diterpenoids from *Sarcodon scabrosus*, Biosci. Biotechnol. Biochem. 68 (6) (2004) 1362–1365.
[13] H.Y. Tang, et al., Structure diversity, synthesis, and biological activity of cyathane diterpenoids in higher fungi, Curr. Med. Chem. 22 (19) (2015) 2375–2391.
[14] J. Frelek, W.J. Szczepek, $[Rh_2(OCOCF_3)_4]$ as an auxiliary chromophore in chiroptical studies on steroidal alcohols, Tetrahedron Asymmetry 10 (8) (1999) 1507–1520.
[15] M. Gerards, G. Snatzke, Circular dichroism, XCIII determination of the absolute configuration of alcohols, olefins, epoxides, and ethers from the CD of their "in situ" complexes with $[Rh_2(O_2CCF_3)_4]$, Tetrahedron Asymmetry 1 (4) (1990) 221–236.
[16] S. Kasibhatla, B. Tseng, Why target apoptosis in cancer treatment? Mol. Cancer Ther. 2 (6) (2003) 573–580.
[17] J. Han, et al., Anti-inflammatory and cytotoxic cyathane diterpenoids from the medicinal fungus *Cyathus africanus*, Fitoterapia 84 (2013) 22–31.
[18] S. Elmore, Apoptosis: a review of programmed cell death, Toxicol. Pathol. 35 (4) (2007) 495–516.
[19] J.M. Matés, F.M. Sánchez-Jiménez, Role of reactive oxygen species in apoptosis: implications for cancer therapy, Int. J. Biochem. Cell Biol. 32 (2) (2000) 157–170.
[20] D.N. Dhanasekaran, E.P. Reddy, JNK signaling in apoptosis, Oncogene 27 (48) (2008) 6245–6251.
[21] D.S. Goodsell, The molecular perspective: Bcl-2 and apoptosis, Oncologist 7 (3) (2002) 259–260.
[22] A. Gross, J.M. McDonnell, S.J. Korsmeyer, BCL-2 family members and the mitochondria in apoptosis, Genes Dev. 13 (15) (1999) 1899–1911.
[23] Y. Tsujimoto, Role of Bcl-2 family proteins in apoptosis: apoptosomes or mitochondria? Genes Cells 3 (11) (1998) 697–707.
[24] J.M. Adams, S. Cory, The Bcl-2 protein family: arbiters of cell survival, Science 281 (5381) (1998) 1322–1326.
[25] M. Marani, et al., Identification of novel isoforms of the BH3 domain protein Bim which directly activate Bax To trigger apoptosis, Mol. Cell. Biol. 22 (11) (2002) 3577–3589.
[26] S. Haupt, et al., Apoptosis – the p53 network, J. Cell Sci. 116 (Pt 20) (2003) 4077–4085.
[27] J.S. Fridman, S.W. Lowe, Control of apoptosis by p53, Oncogene 22 (56) (2003) 9030–9040.
[28] M.E. McCurrach, et al., bax-deficiency promotes drug resistance and oncogenic transformation by attenuating p53-dependent apoptosis, Proc. Natl. Acad. Sci. 94 (6) (1997) 2345–2349.
[29] A. Basu, S. Haldar, The relationship between Bcl2, Bax and p53: consequences for cell cycle progression and cell death, Mol. Hum. Reprod. 4 (12) (1998) 1099–1109.
[30] A.L. Genestier, et al., *Staphylococcus aureus* Panton-Valentine leukocidin directly targets mitochondria and induces Bax-independent apoptosis of human neutrophils, J. Clin. Investig. 115 (11) (2005) 3117–3127.
[31] T.R. Wilson, et al., Combined inhibition of FLIP and XIAP induces Bax-independent apoptosis in type II colorectal cancer cells, Oncogene 28 (1) (2009) 63–72.
[32] B.B. Chandrika, et al., Bax deficiency mediated drug resistance can be reversed by endoplasmic reticulum stress induced death signaling, Biochem. Pharmacol. 79 (11) (2010) 1589–1599.
[33] S. Orrenius, V.O. Kaminskyy, B. Zhivotovsky, Autophagy in toxicology: cause or consequence? Annu. Rev. Pharmacol. Toxicol. 53 (2013) 275–297.
[34] D.J. Klionsky, et al., Guidelines for the use and interpretation of assays for monitoring autophagy, Autophagy 8 (4) (2012) 445–544.
[35] K. Sasaki, et al., Chloroquine potentiates the anti-cancer effect of 5-fluorouracil on colon cancer cells, BMC Cancer 10 (2010) 370.
[36] A.N. Hale, et al., Autophagy: regulation and role in development, Autophagy 9 (7) (2013) 951–972.
[37] P. Codogno, A.J. Meijer, Atg5: more than an autophagy factor, Nat. Cell Biol. 8 (10) (2006) 1045–1047.
[38] S. Luo, D. Rubinsztein, Atg5 and Bcl-2 provide novel insights into the interplay between apoptosis and autophagy, Cell Death Differ. 14 (7) (2007) 1247–1249.
[39] S. Yousefi, et al., Calpain-mediated cleavage of Atg5 switches autophagy to apoptosis, Nat. Cell Biol. 8 (10) (2006) 1124–1132.
[40] S. Yousefi, H.U. Simon, Apoptosis regulation by autophagy gene 5, Crit. Rev. Oncol. Hematol. 63 (3) (2007) 241–244.